
IOWA STATE UNIVERSITY

FLIGHT READINESS REPORT 2014



CySLI

TABLE OF CONTENTS

INTRODUCTION	3
EXECUTIVE SUMMARY	4
SAFETY AND MISSION ASSURANCE	4
DESIGN FEATURES OF PAYLOAD	5
DESIGN FEATURES OF ROCKET	17
ANALYSIS OF EXPECTED PERFORMANCE	22
CONCLUSION	24
REFRENCES	24
BUDGET	25

INTRODUCTION

School Name: Iowa State University

Team Name: CySLI

Faculty Advisor:

Matt Nelson, Make to Innovate Project Coordinator

Phone: 515-294-2640

Email: mnelson@iastate.edu

Team Leader:

Jacob Harry

Cell: (515) 321-6785

Email: jwharry@iastate.edu

Team Members:

Ryan Smelser (Payload Team Co-Leader)

Luis Dietsche (Payload Team Co-Leader)

Matt Dickinson

Brandon Bay

Jordan Mathews

Caroline Pereira

Andrew Jirik

Connor Coffey

Christian White

Dan McDonald

Caleb Burt

EXECUTIVE SUMMARY

The competition directive called for determining velocity vs. altitude and acceleration vs. altitude using multiple measurement methods. The intention is to allow teams to cross-validate data between systems and potentially identify certain advantages or shortcomings of the technologies used. The CySLI payload includes a barometer, accelerometer, and GPS device working in tandem with a Raspberry Pi computer. The logging barometer measures pressure, which is converted into an altitude and numerically differentiated post-flight in MATLAB to obtain velocity and acceleration values. The accelerometer data will be recorded and evaluated with particular focus on examining the Euler Angle orientations of the rocket. The GPS will send geographic coordinates and altitude to the Raspberry Pi and will store them for post-flight velocity and acceleration analysis. In addition, the Pi will be utilized in the control of a variable-drag air brake system.

The CySLI rocket was designed and constructed to achieve a 3000-foot apogee while satisfying the WSGC Competition limitations. The rocket diameter is 6 inches in diameter and 83.5 inches in length with a stability margin of 1.4 calibers. Phenolic tubing and fiberglass were used as primary materials in the rocket and were specifically selected based on parameters of durability, density, aesthetics and cost. After incorporating masses from the payload and air brake systems, a K400 motor was selected to bring the rocket apogee into the “braking range” of the vehicle.

The expected performance of the rocket was analyzed using two computer software programs: OpenRocket and RockSim Pro. OpenRocket provided a good starting place for the team and allowed for basic approximations of the apogee altitude. RockSim Pro is advantageous in that it utilizes uncertainty calculations to provide a more robust estimate of potential rocket trajectories. The projected apogee of the rocket is 3200 feet, which is above the objective altitude of 3000 feet. However, with the implementation of a custom air brake system, increased drag after motor burnout will result in an apogee much closer to the 3000 feet. Air brakes cannot be simulated with either of the aforementioned software, so a new technique needed to be used.

The air brake system was modeled in a computational fluid dynamics (CFD) program called Star-CCM+. By using CFD, an estimate of the increased drag caused by the deployed air brake flaps can be used to more accurately characterize the flight performance of the rocket. Ultimately, the designed rocket, payload and air brake will result in a successful report of velocity and acceleration from multiple systems and a rocket apogee of 3000 feet.

SAFETY AND MISSION ASSURANCE

CySLI has gone through many lengths in order to ensure the safety and mission assurance of its high-powered rocket. Many crucial parts of the rocket have been quality checked and tested

to ensure they properly work throughout launch. The air brakes have been tested through their full range of motion to verify that none of the individual brakes become stuck and offset the center of pressure from the rocket. In addition, a full electronics test was run to verify that the software and hardware of the air brakes module communicate properly.

The structural aspects of the fin connections, shear pins and rivets, motor mount, and overall body tube were analyzed for any improper epoxy joints or cracks to ensure structural integrity. The mounting of the various electronic modules on the payload sled were also checked to ensure that no electronics become loose or wires disconnect during the acceleration phases of the rocket.

Safety is also an important issue whenever high-powered rocketry is involved and one that CySLI takes very seriously. All team members are required to sign a safety agreement to follow all safety regulations set by the NAR rocket code. Before any launch, the team will be fully briefed on how the rocket will be tested, the outcome of the testing, and the NAR High Powered Safety Code will be reviewed to ensure that the team is within safety guidelines.

The team will then meet with Mr. Gary Stroick, who has been involved in high-powered rocketry since 1998 and is certified Level 3 with the Tripoli Rocketry Association. Mr. Stroick will thoroughly analyze the rocket to ensure it is properly set up for launch and that no mishaps will occur. In addition, Mr. Stroick will review our checklists for the launch to verify all items are being checked and that everyone understands their jobs.

During launch, every team member will have a specific job with someone to oversee them. This will ensure no mishaps or mistakes will be made and that there is no confusion between team members on who is assigned what task. At the time of launch, only one team member will be in charge of the launch controller and will audibly yell out a countdown before the launch ignition key is pressed.

Under no circumstances will CySLI tolerate any deliberate or unintentional failure to follow the NAR High Powered Safety Code and will severely warn or disqualify those who do from the team. Because of CySLI's high quality assurance standards, its many tests of the rocket subsystems, and its high standard of safety, we are certain we can complete this mission without failure.

DESIGN FEATURES OF PAYLOAD

ACCELEROMETER/GYROSCOPE AND EULER ANGLES

One of the flight performance sensing devices in the electronics bay is a combination accelerometer and gyroscope module. The L3GD20 gyroscope uses the law of conservation of angular momentum to determine the angular velocity about all three of the axes defined on the module. The LSM303DLHC chip is also contained in this device and consists of an accelerometer and magnetometer, both defined along the same three axes as the gyroscope. The accelerometer is a micro electro-mechanical system (MEMS), meaning that it uses capacitance to create a voltage proportional to the deflection of a small beam inside the device caused by

acceleration. The magnetometer determines the strength of magnetic fields in the three axes. These readings can supplement the gyroscope and be combined using a filter to have accuracy over a larger spectrum of rotation frequencies.

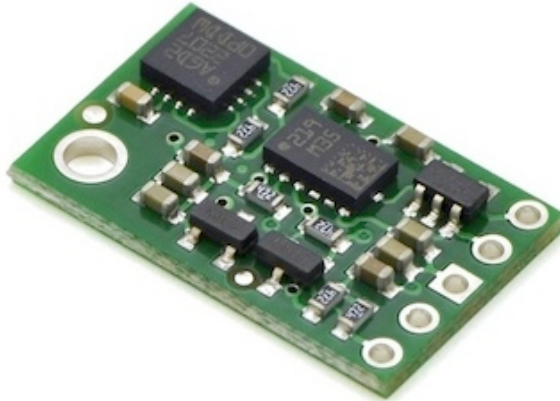


Figure 1: The LSM303DLHC chip and L3GD20 gyroscope (HobbyTronics)

When analyzing the vehicle's dynamics, one important factor considered is its orientation. Therefore, the onboard gyroscope is used to track the angles of the rocket's orientation from a body frame of reference. In order for the accelerometer data to be made useful for detailed analysis, the transition from an onboard perspective to an Earth-centered or global frame must be made. To accomplish this feat, one must take measured body frame acceleration vectors at each instance, then multiply them by rotation matrices to obtain global frame acceleration vectors.

Since the team will not need this data to be analyzed real-time while the rocket is flying, MATLAB code has been written to take the measurements of the accelerometer and convert them as previously described. Plots of velocity and acceleration versus altitude will then be generated by integrating the global frame accelerations.

BAROMETER

For the purpose of obtaining a secondary set of flight information, the team chose to use a barometric altimeter. The specific model selected was a ZLog-7 Recording Altimeter which is intended for high-altitude experiments and should work for our purposes. The barometer captures the atmospheric pressure and temperature once per second and uses the standard atmosphere and isentropic relations to calculate the altitude. Using a program created in MATLAB, the altitude versus time graph can be easily obtained. Differentiation of this data will allow for the plotting of speed and acceleration versus time. We can compare these results to those obtained by the other systems, which have a much higher data capture rate and generally lower error. A conclusion can then be made regarding critical frequency and confidence bounds where data no longer accurately portrays actual flight performance.

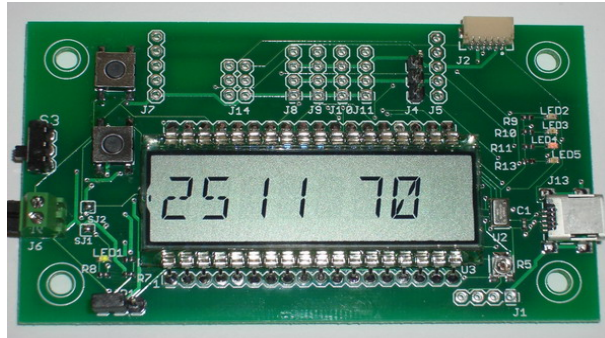


Figure 2: The ZLog-7 barometer (Hexpert Systems)

GLOBAL POSITIONING SYSTEM

The Global Positioning System measures the position and altitude of the rocket using satellites. The team's chosen receiver, the Adafruit Ultimate GPS Breakout, will obtain the signals from satellites, which know and transmit their precise position and time. That is, the GPS receiver will obtain a two-dimensional fix using the signals from three satellites, and from a fourth satellite, its altitude. With this data and an update rate of ten Hertz, the team will accurately differentiate the altitude with respect to time to find vertical velocity and acceleration.

Without a known function of time for altitude, we are using the forward, backward and central difference formulae. These estimate the derivative by finding the slope between the data points. For the forward difference formula, the slope will be found using rise over run of the first two data points; backward difference is similar. For the central difference formula, to estimate the velocity for a given data point between the beginning and final data points, the data points before and after the desired data point will be connected with a secant line. Hence, this slope will give a better approximation here than using formulae similar to the forward or backward difference formulae.

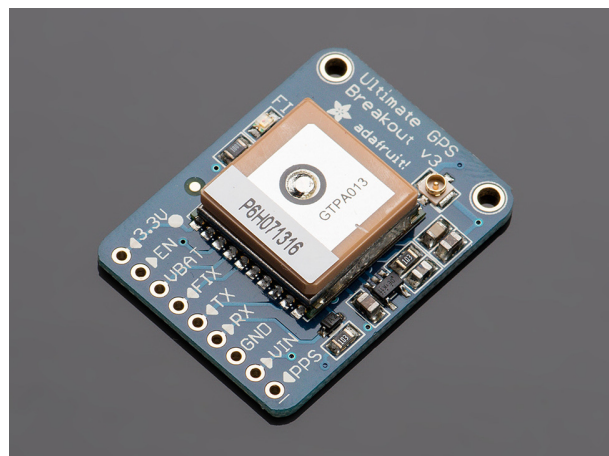


Figure 3: The Adafruit Ultimate GPS Breakout (Adafruit)

AIR BRAKE SYSTEM OBJECTIVE

The objective of the air brake system is to provide a variable amount of drag force after motor burnout to control the deceleration of the rocket in order to achieve the desired apogee of 3000 feet. The following air brake system was designed to minimize moving parts, as well as for cost effectiveness and ease of manufacturing.

MECHANICAL DESIGN

A 3D model of the interior portion of the air brake assembly is shown in Figure 4. The main air brake system components consist of two mounting plates, four air brake flaps, an air brake arm and a servo. Air brake flaps are mounted between the lower and upper mounting plate using four $\frac{1}{4}$ " fasteners. Brass sleeve bearings were inserted between each air brake flap and $\frac{1}{4}$ " fastener to decrease friction between the two surfaces. An aluminum dowel pin was inserted in each air brake flap. This dowel pin is used to slide inside the arm slots of the air brake arm. The slots on the air brake arm are designed to radially deploy the air brake flaps. The air brake arm is mounted to a high-torque servo, which is attached with four #6-32 fasteners to the upper mounting plate. To attach the air brake system to the interior of the rocket, the lower mounting plate is attached using four $\frac{1}{4}$ " fasteners on a permanent wood bulkhead located inside the rocket coupling tube. This will allow the air brake system to be removed from the rocket if needed.

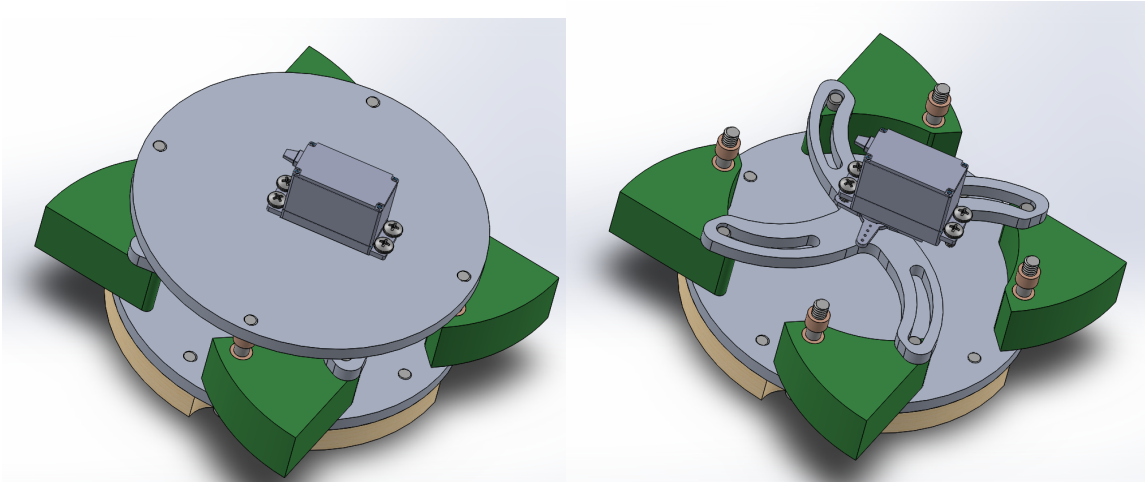


Figure 4: Interior Parts of Air Brake Model with the Upper Plate (Left) and without the Upper Plate (Right)

The air brake assembly will be attached to the rocket using a coupling tube. In Figure 5, the brown tube is a standard coupling tube, and the white tube has similar dimensions as the rocket airframe. The left model shows the air brake flaps in the fully closed position. This position will be used while the motor is burning or when no additional drag is needed. The right model shows the air brake flaps in the fully deployed position, which will provide the maximum amount of drag.

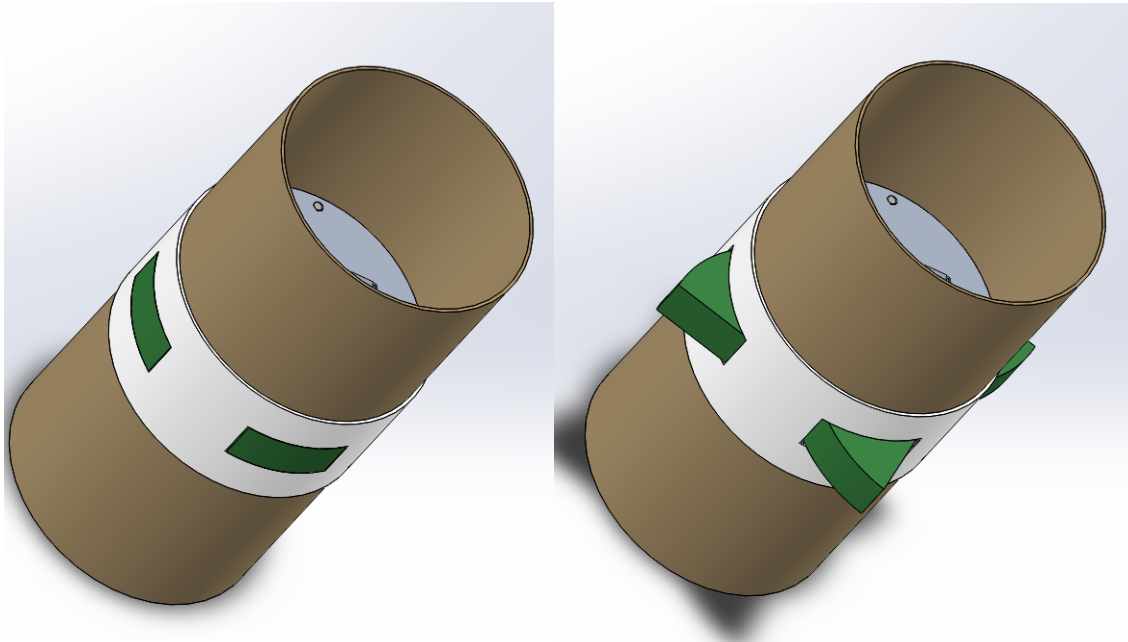


Figure 5: Air Brake Model Showing Fully Closed (Left) and Fully Deployed (Right) Positions

MANUFACTURING

The mounting plates, air brake arm, and air brake flaps were all created using the manufacturing equipment available at Iowa State University's machine shops. The two mounting plates and the air brake arm each began as 6"x6"x1/4" 6061 aluminum plate stock. Each mounting plate was turned on a lathe to an outside diameter 0.02 inches less than the rocket's coupler tube, allowing the two plates to fit inside the coupler tube. The holes and rectangular pocket were made using a vertical mill, and the holes needed to be tapped were done by hand. To create the air brake arm a .dxf file was created using the 3D model of the part. The .dxf file was uploaded to the vertical mill computer, allowing the mill to follow the path of the slots and outside contour of the part. To create the air brake flaps, a .stl file was created using the 3D model of the air brake flap part. Using the .stl file, the air brake flaps were 3D printed using ABS plastic.

ROCKET KINEMATICS DURING COAST AND COMPUTATIONAL FLUID DYNAMICS

In order to predict apogee after burnout of the rocket with air brakes extended, it was necessary to derive kinematic equations from Newton's Second Law. From summing the forces in the vertical, or **z**-direction, we obtain the equation $ma_z = -mg - \beta V^2 \sin(\alpha)$ (1), where m is the mass of the rocket and payload after burnout, a_z is the net acceleration along the **z**-axis, g is the acceleration due to gravity, β is the dimensional drag coefficient (DDC), V is the speed, and α is

the angle between the rocket and the horizon. We chose this equation to model the drag we expect as the rocket travels subsonically at a maximum speed of Mach 0.4. The angle was included because we wanted to account for wind and other effects. Below is a depiction of the rocket during coast to apogee:

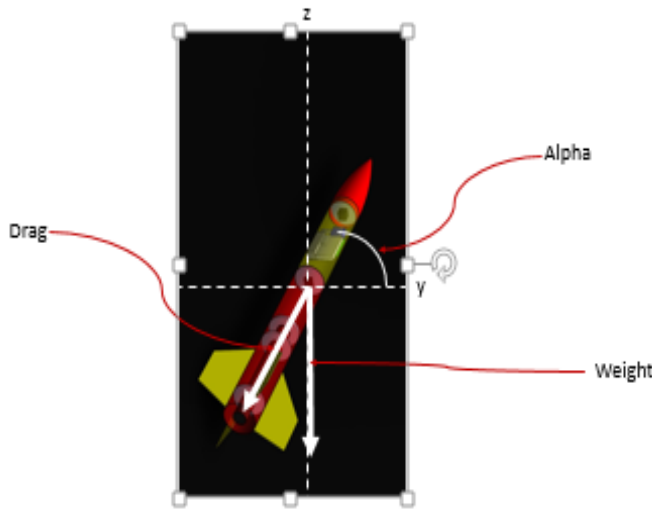


Figure 6: Forces acting on the rocket after burnout with an angle

Integrating equation (1) twice, using the chain rule to find the z -component of velocity, yields the apogee as a function of speed at an altitude after burnout:

$$h_{apo} = -(m \sin(\alpha)/2\beta) \ln((\beta V_{y,apo}^2 \sin(\alpha) + W)/(\beta V_{alt}^2 \sin(\alpha) + W)) + h_{alt} \quad (2)$$

where h_{apo} is the apogee altitude, $V_{y,apo}$ is the residual horizontal speed at apogee, W is the weight of the rocket and payload, V_{alt} is the speed at any altitude after burnout but before apogee, and h_{alt} is any altitude after burnout but before apogee. For quick verification of this result, we referenced an online resource which gives apogee of the rocket in one dimension (Culp):

$$h_{apo} = -(m/2\beta) \ln(W/(\beta V_{alt}^2 + W)) + h_{alt} \quad (3)$$

If $\alpha = 90^\circ$ in equation (2), then there is no horizontal speed at apogee, and equation (2) is identical to equation (3).

Since horizontal speed appears in equation (2), its derivation was required. Summing the forces in the horizontal, or y -direction, gave $m a_y = -\beta V^2 \cos(\alpha)$ (4). Solving for time to apogee from an altitude by integrating equation (1) with respect to it and substituting the result into the time integration of equation (4) produced the following equation for horizontal speed:

$$V_{y,apo} = [1/V_{y,alt} + (\beta/(mcos(\alpha))) \sqrt{(msin(\alpha)/(g\beta)} \tan^{-1}(\sqrt{(\beta/(mgsin(\alpha))} V_{z,alt})]^{-1} \quad (5)$$

where $V_{z,alt}$ is the vertical velocity at any altitude after burnout but before apogee. For simple verification, we utilized dimensional analysis. The DDC has units of $\frac{[M]}{[L]}$ which makes the product $(\beta/(mcos(\alpha))) \sqrt{(msin(\alpha)/(g\beta)} \tan^{-1}(\sqrt{(\beta/(mgsin(\alpha))} V_{z,alt})$ have units of $\frac{[T]}{[L]}$. When

equation (5) is taken to the inverse power, then we arrive at the correct units for speed of $\frac{[L]}{[T]^2}$. The argument inside inverse tangent must be dimensionless, and it is upon inspection. Finally, substituting equation (5) into equation (2) allows for reasonable predictions of apogee at any point along the coasting trajectory. A plot of apogee versus DDC follows:

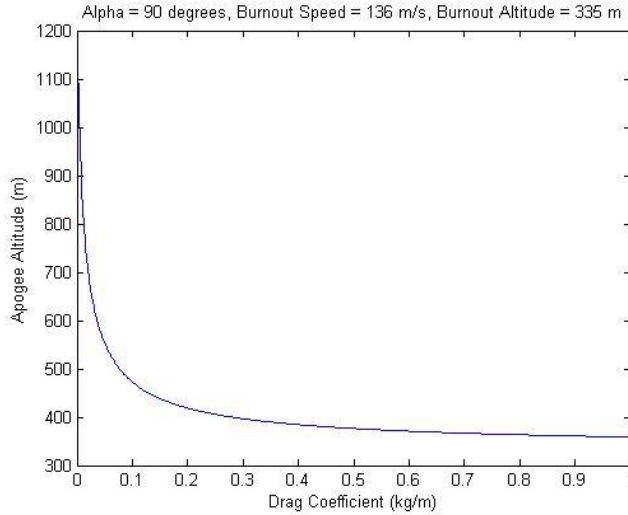


Figure 7: Theoretical apogee versus DDC

The next step taken to engineer the air brakes was Computational Fluid Dynamics (CFD) of various modes at various speeds. We arbitrarily chose five evenly spaced modes of extension, ranging from zero to full extension. Then we numerically integrated the antiderivative of equation (1) and found that 90% of apogee was achieved during speeds greater than 40 m/s. Thus, we chose five evenly spaced test speeds ranging from 40 m/s to 157 m/s, the earlier prototype's burnout speed.

Much work went into modeling each simulation in Star-CCM+, the CFD software available to our team through Iowa State University. Not only did we teach ourselves how to use the software through online tutorials, which we received from the university, but we also encountered many minor issues along the way--importing a compatible and accurate version of a SolidWorks model prevailed as the greatest problem. Other issues included large amounts of computation times due to inefficiencies in our modeling, as well as understanding the correct physical model to use for the fluid flow.

An example of the results we obtained is displayed in Figure 8. It is a force report of normal and shear forces acting on the labeled parts. The monitor value at the bottom of Figure 8 is the total drag, and setting this equal to the DDC times the speed squared allowed us to solve for the DDC.

157 m/s
 Reference Pressure = 0.0 Pa
 Direction: [1.0, 0.0, 0.0]
 Coordinate System: Laboratory
 Vectors

Part	Pressure(N)	Shear(N)	Net(N)
Default	[6.099492e+01, -2.576050e+00, -2.610979e+00] [2.891846e+01, 1.132802e-01, -7.711663e-02] [8.991338e+01, -2.462770e+00, -2.688096e+00]		
Totals:	[6.099492e+01, -2.576050e+00, -2.610979e+00] [2.891846e+01, 1.132802e-01, -7.711663e-02] [8.991338e+01, -2.462770e+00, -2.688096e+00]		
Component in direction: [1.000000e+00, 0.000000e+00, 0.000000e+00] in Laboratory coordinate system			
Part	Pressure(N)	Shear(N)	Net(N)
Default	6.099492e+01	2.891846e+01	8.991338e+01
Totals:	6.099492e+01	2.891846e+01	8.991338e+01

Monitor value: 89.91337950736421

Figure 8: Solving for the DDC in this example gives
 $\beta = 89.9134 \text{ N}/(157 \text{ m/s})^2 = 0.00365 \text{ kg/m}$

After clearing obstacles with some help from faculty members, we began to achieve reasonable results from the simulations. In order to account for the difference between the no-extension mode DDC in Star-CCM+ and the one from OpenRocket, we simply added the difference to every mode's DDC. This was a high estimation, but we still found the first version of our air brakes were not going to have a great effect on producing drag. Hence, we maximized the surface area of the air brakes and reran the simulations.

Due to our commitment to realistically controlling the air brakes, we pushed to settle the discrepancy between the no-extension mode DDC in Star-CCM+ and the one in OpenRocket. After some debating, we realized our models in Star-CCM+ lacked a characteristic height for surface roughness. Once we applied the matching 150 micrometer characteristic height and ran the simulations, we got the no-extension mode DDC's to match, and found that our air brakes would decrease apogee by a maximum amount of 180 feet (55 m) for our prototype rocket. A plot of apogee versus the range of DDC's we expected to see for our first prototype is included below:

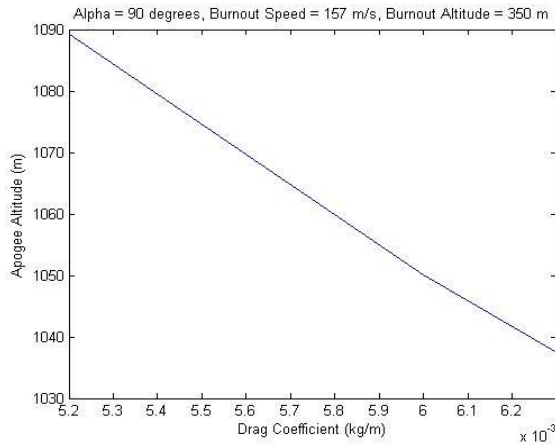


Figure 9: Expected apogees and DDC's obtained from Star-CCM+

Since 180 feet was not going to be a large enough decrease, we added mass to our rocket to get a more workable range of apogees. The next figure shows our finalized apogee projections:

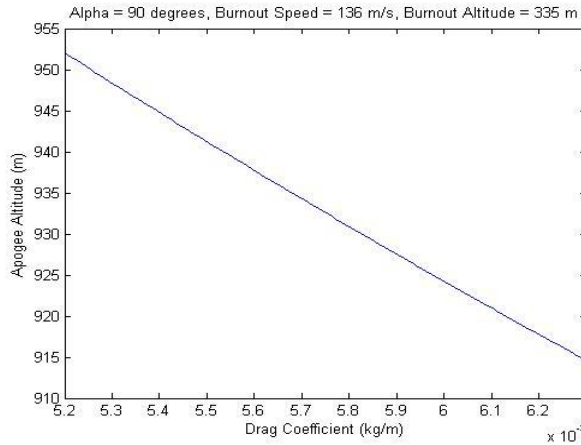


Figure 10: New model predictions show a possible reduction of 124 ft (38 m) to 2999 ft

Due to statistical variation of impulse of rocket motors, we believe this new model will give us the best chance at staying within the 3000-foot mark. Notice as well that Figure 10 does not account for weather effects or arcing of the rocket. If we let the angle vary by plus or minus ten degrees, then we have a greater range of apogees, which cross the target apogee, as shown in Figure 11:

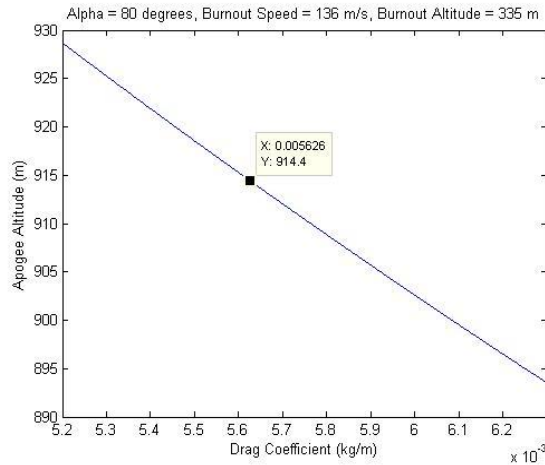


Figure 11: An example of how wind or arcing will affect the range of predicted apogeies. The target apogee of 914.4 meters is shown.

In conclusion, variations such as the one in Figure 11, depict how the current model has a good chance of exactly achieving 3000 feet due to the maximized surface area of the air brakes, heavier rocket, and avionics which have all implemented the theory discussed.

AVIONICS AND AIR BRAKE CONTROL

The air braking system mentioned above is controlled using a closed loop digital control system. A Raspberry Pi computer, shown below in Figure 12, serves as the data processor and system controller. This device was chosen due to its affordability, ability to interface with necessary flight data equipment, impressive processing speed, and many advantages over simpler controllers. The diagram below encompasses all of the onboard avionics, with the exception of the stand-alone barometric altimeter.

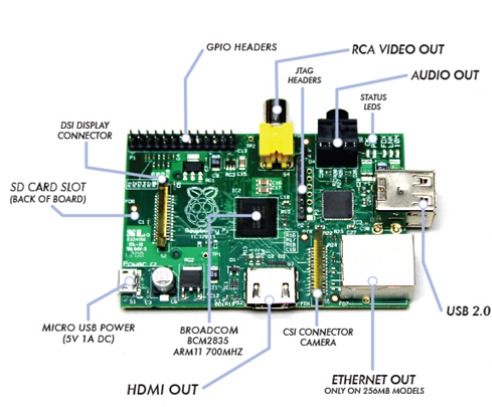


Figure 12: Raspberry Pi Computer (Murray)

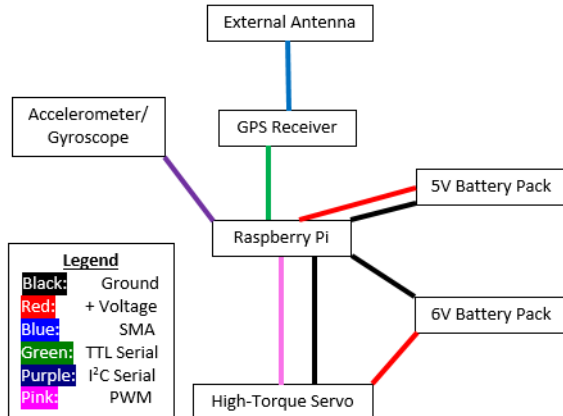


Figure 13: Avionics System Diagram

AVIONICS INTERFACING

Four connections define the I²C serial interface between the accelerometer/gyroscope module and the Raspberry Pi. First, power is supplied to the module at five volts directly from the general purpose input/output (GPIO) headers of the Raspberry Pi. Next, a bidirectional SDA line carries the data pattern and acknowledgment of successful communication. Finally, a unidirectional SCL line carries three dimensions of acceleration data, gyroscopic rotation rate data, and magnetometer data. Pre-defined system gains are used for both devices to convert raw data into standard units once it is received.

Communication is made between the Raspberry Pi and global positioning satellites through the GPS module. In order to reduce error and the amount of time needed to obtain a fix, an external antenna was attached to the module at the u.FL port with the use of an SMA adapter cable. The TTL serial interface between the GPS chip and the Raspberry Pi again uses four connections on the GPIO headers, including the same five-volt power line and ground. Additionally, this interface separates transmission and reception into two lines. The transmission line is used to send commands to the module, specifically to increase update frequency and baud rates. At the same time, the reception line carries both GPS data and sentences responding to commands.

The mechanical air braking system is physically connected to the avionics using a standard high-torque servo. The decision to power the servo with a six volt battery separate from the Raspberry Pi power source was made for multiple reasons. Most importantly, speeds in excess of Mach 0.4 at motor burnout induce loads on the air brakes. This will cause friction between the brake flaps and the base plate, as well as resistance to the retraction of the flaps. Giving the servo a higher voltage will maximize possible torque, while separating it from the Raspberry Pi power will prevent high current draws from restarting the device and killing the programs. Control of the servo is completed using pulse width modulation (PWM), where the duration of the pulses for this application range from approximately 1.45 to 1.75 milliseconds on a 20 millisecond cycle. However, because the Raspberry Pi generates signals on the GPIO pins based on the device's electrical ground, simply connecting the servo control line to the PWM pin would result in an unrecognizable signal. Instead, the servo battery and servo motor must both be connected to the same ground as the Raspberry Pi. This was accomplished by simply connecting both grounds to the GPIO ground, the six-volt power line directly to the servo, and the PWM GPIO pin directly to the servo. Finally, because forces will exist acting against the desired position of the servo at virtually all times during flight, the PWM signal must be constantly sent. In order to accomplish this while leaving the central processing unit of the Raspberry Pi free to process data, the software initializes GPIO control via direct memory access (DMA). An open source software package called "PIGPIO" was utilized to execute this process.

SOFTWARE LOGIC

Because of the complicated nature of calibrating and filtering accelerometer and gyroscope data, as well as the detrimental effects of double integration on small accelerometer errors, the GPS module was chosen to be the sensor used for air brake control. Therefore, the data processing software for the accelerometer/gyroscope unit was quite simple. Both the acceleration and rotation rate data are received as packets of six bytes of data, two for each axis. An approximate conversion factor is applied in a C program before writing the values to an output file. Additionally, the internal clock of the Raspberry Pi is used to determine elapsed time in each iteration, which is also written to the file.

An open source GPS Daemon is loaded onto the Raspberry Pi and is used to translate serial data packets into usable values. In addition, a Python class written by the manufacturer of the GPS chip utilizes the Daemon to create an object instance, in which object parameters are the different parts of the report. With this, the air brake control software could be written under the premise that latitude, longitude, ground speed, and climb rate are floating point numbers.

Due to the variance of rocket motors, predicting an apogee altitude at any time before motor burnout is virtually impossible. Therefore, it is desired for the brakes to only be deployed from burnout to apogee. In order to achieve this, the flight was broken up into five stages, which are enumerated in the code and described below. Time, latitude, longitude, ground speed, altitude, and climb rate are still collected and written ten times per second at all stages until the rocket is on the ground

The pre-launch stage is theoretically defined as the time from when the program is started to the time of launch. However, because there is no need to know exactly when launch occurs, the transition to the burn stage is defined in the software as the point when the rocket is 25 meters above the starting altitude. During this stage, the program simply waits for launch.

The burn stage can be theoretically defined as the time when the motor is burning. The transition out of this stage occurs at maximum velocity, because vertical acceleration becomes negative when thrust ends. Therefore, during this stage, the program watches for the velocity to decrease. In order to account for possible error during the burn stage, velocity must be five percent less than maximum velocity yet experienced to move to the drift-up stage.

The drift-up stage is defined theoretically as the period of time after the motor has burned out until apogee is reached. This is the only stage in which the program predicts apogee altitude and uses it to control the air brakes. First, dimensional drag coefficient is determined using a vertical force balance with the hard-coded mass and numerical derivative of climb rate. Next, horizontal velocity at apogee is predicted, allowing for the prediction of apogee altitude, as discussed previously. The signal pulse widths corresponding to fully retracted and fully extended configurations of the air brake system are determined prior to launch and stored in the program. If the predicted apogee is greater than desired apogee and the air brakes are not fully deployed, then the servo pulse width will be incremented by one-tenth of the entire range of the brakes. Conversely, if predicted apogee falls below desired apogee and the brakes are not fully retracted, the servo pulse width is marginally decremented. The same logic applied to climb rate

to determine when burn is complete is applied to altitude to determine when the rocket is finished drifting up. At this point, transition is made to the next stage.

The float-down stage is theoretically defined as the time from apogee to touchdown. During this stage, the program simply records data and watches for the magnitude of climb rate to drop under 1.0 m/s while altitude is within 50 meters of starting altitude. Because ground contact is predicted to occur at a much higher speed, this should indicate the precise time when touchdown occurs. At this point, the grounded stage is entered and the program is ended.

DESIGN FEATURES OF ROCKET

The objective of CySLI's rocket design is to build a launch vehicle that is within the constraints of the competition, with special consideration paid to the ease of construction and assembly of the rocket. In order to improve construction efficiency, yet still assure team member participation, sub-teams were created to work on certain tasks. This maximized the work completed in a given lab session and gave team members with less experience a chance to build confidence throughout the rocket construction process. In addition, a small-scale rocket, with a comparable stability margin and geometry, was constructed and launched in December. Although the competition-scale design is far more elaborate, a great deal is gained from seeing the start to finish process of building a rocket of any scale and learning the critical design parameters required to do so. The small-scale launch was beneficial in that, by undergoing this task immediately, team members were more educated and further able to contribute to the discussion of designing and constructing the large rocket.

The rocket body tubing is 6 inches in diameter to accommodate for the number of electronics placed in the payload bay as well as allow for proper deployment of the drogue and main parachutes. There are three sections of the phenolic body tubing, the foreword section is 20.5 inches long, the middle section is 12.5 inches long, and the aft section is 23.5 inches long. The sizing allows enough room for two parachutes each attached to 20 feet of Kevlar shock cord.



Figure 14: Andrew Finishing Construction of Small-Scale Rocket

The parachute dual-deployment system will consist of a drogue and main parachute, the sizes of which were determined by the total mass of the rocket. The drogue chute is 24 inches in diameter and will be deployed near apogee via altimeter-based black powder ignition with a secondary charge detonating through the timing delay of the motor. This deployment altitude ensures that the drogue chute will encounter the smallest amount of loading, minimizing the possibility of a torn chute. This smaller drogue is designed to lower the altitude of the rocket in a steady and controlled manner. The larger main parachute, 96 inches in diameter, will be deployed around 800 feet with the detonation of black powder charges on an electric signal from the altimeter. The main parachute will slow the rocket down to a safe descent speed of 20 feet per second, which will allow the rocket to impact the ground and still retain its structure and overall reusability.

The payload bay and air brake system are designed in two separate 12-inch coupling tubes that connect the three sections of the rocket. The payload will be used to hold the rocket altimeters, altimeter batteries and the electronics used to complete the WSGC Competition directive. The payload bay will be enclosed with removable plywood bulkheads; these will provide protection from any explosive black powder residue that may result from deployment of the parachutes. The nosecone will be held to the upper section by shear pins and will tear off with main parachute deployment. Removable rivets will be used to connect the upper and middle sections to the payload bay. On the other hand, the air brake is designed to be riveted to the middle section, but be connected with shear pins to the lower section of the rocket, allowing for the initial drogue chute deployment. The payload and air brake system will be connected with wires through the entirety of the flight; this aspect of the design was intended to minimize separation complications.

The fins and nosecone are both made of a stronger, denser fiberglass material. The nosecone is 24 inches in length with a 4-inch shoulder. This component undergoes some of the

most violent conditions of any part on the rocket, and fiberglass is one of the most durable solutions of any material. The fiberglass is also optimal for use in the fins because of its high strength to weight ratio when compared to materials of similar densities. In addition, fiberglass is resistant to moisture and corrosion, the latter would be especially important because of the fin proximity to the caustic fumes of the rocket exhaust. Although fiberglass is more expensive than some other materials, it is used in locations where retaining shape and aerodynamic stability is non-negotiable. In these areas of the rocket, structural and aerodynamic integrity take precedence over cheaper solutions.

After all the rocket components with the appropriate materials were determined, the fully loaded mass of the rocket was determined to be 20 lbs. with stability of 1.4 calibers preflight. Of the eight potential motors to use in the vehicle launch, the 54 mm Cesaroni K400 was selected. With an average thrust of around 400 newtons and a total impulse of 1600 newton-seconds, the simulations with the K400 yielded a rocket apogee of approximately 3200 feet.

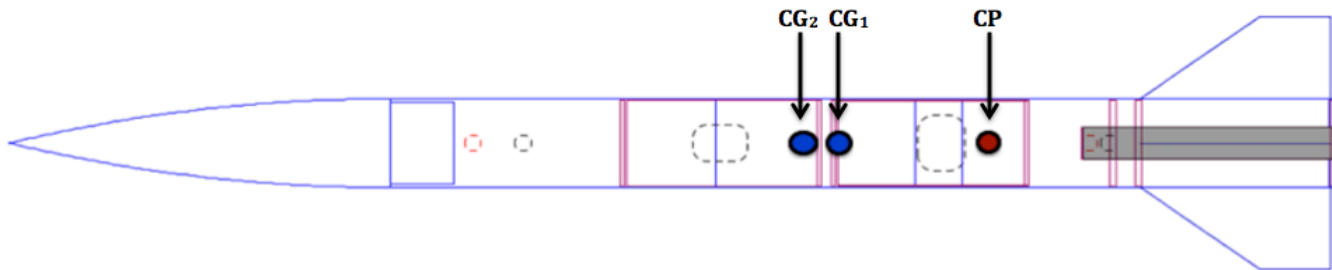


Figure 15: Location of Rocket Center of Gravity and Center of Pressure: CG₁ = 52.1 in. (Before Motor Burnout), CG₂ = 49.3 in. (After Motor Burnout), CP = 61.7 in.

In the design, there were several risk mitigation techniques used to reduce the likelihood of dangerous events. One of the techniques used in the design is the utilization of multiple altimeters in the main parachute deployment event. At that time in the launch, the rocket was simulated to be traveling at 64 feet per second downward. This speed, upon impact, would not only cause permanent damage to the rocket, but it would also be dangerous for bystanders of the launch. The second altimeter is wired to a secondary black powder charge of equal mass, that would diminish the risk of the main parachute not deploying.

An additional risk mitigation technique used in the design and construction process is the testing of black powder charges. The amount of black powder in the charges is directly related to the volume of the gas expanding in a given body tube section. It is critical to identify the amount of powder mass necessary for a specific rocket configuration. Too little mass will not break the shear pins, while too much powder may crack open the body tubes. The rocket design uses 6 shear pins in each breakaway section; the initial mass was calculated by approximating a lower limit value for the mass from a known black powder explosive calculating spreadsheet. If the

sections did not break apart, small steps were iteratively taken to increase the mass until the shear pins reached their breaking point.



Figure 16: Caleb, Matt, and Brandon constructing the motor mount to be placed in the lower section of the rocket.



Figure 17: Matt using Dremel tool to cut slots in the air brake



Figure 18: Brandon putting finishing touches on the rocket



Figure 19: Finished Painted Rocket in Aerospace Engineering Building

ANALYSIS OF EXPECTED PERFORMANCE

The launch analysis of the rocket can be described as the following. OpenRocket and RockSim Pro were used in the expected performance analysis of the rocket. The launch analysis used the geometry and densities of all the final components in the rocket along with the motor selected for the given launch to attain the following launch parameters. The velocity off the rail was computed to be 32.5 feet per second. This parameter is critical because to ensure stable flight the launch rail exit velocity must be a speed that allows the fins to exert aerodynamic control on the rocket. This aerodynamics control is exerted at the center of pressure location of the rocket. Through the stability analysis performed in the two different software, the relationship between center of gravity and center of pressure was investigated. The stability margin was found to increase from 1.4 to 1.6 calibers as the motor propellant decreased. The mass of the rocket in the lower sections and subsequently allowed for the movement of the center of gravity further towards the nose of the rocket, making it more stable. Additionally, the velocity at motor burnout was calculated to be 475 feet per second.

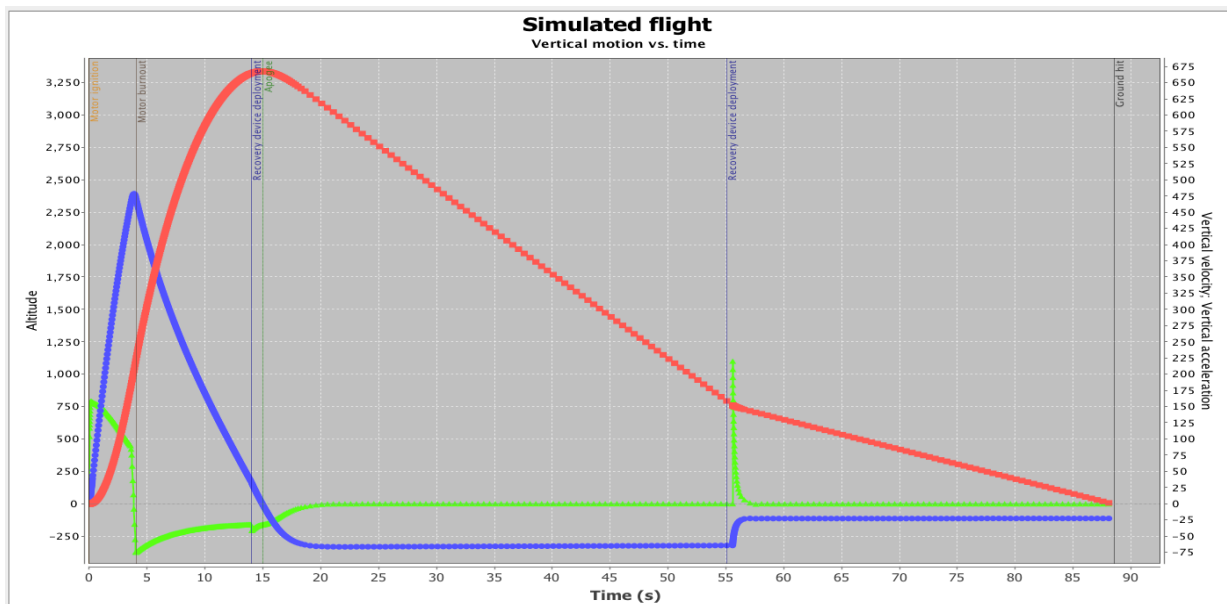


Figure 20: Altitude (Red), Velocity (Blue), Acceleration (Green) vs. Time of Rocket Flight

From this point, two different paths were taken en route to determining rocket apogee. The first path was to allow the simulated flight continue unperturbed using OpenRocket and RockSim. This yielded a maximum altitude of 3180 feet. The second path involved computing the apogee with the additional drag of the air brake system. The equations for flying motions of drag were derived analytically. Using these equations, a code in MATLAB was written to use the motor burnout velocity as an initial condition and calculate the rocket apogee based on the

increased air brake drag. The analysis revealed that the air brake system could decrease the rocket apogee by 180 feet when fully deployed. This is a critical analysis of the rocket flight; a large weight of the team's flight performance is placed on reaching an altitude of 3000 feet. The validity of this analysis will be put to the test in the primary test launch April 12th. Adjustments will be made based on the outcome of this launch yielding a more accurate estimation of the air brake effects on rocket. If the air brakes are indeed effective at diminishing altitude by 200 feet, a rocket apogee of anywhere between 3000 and 3200 feet would be sufficient for reaching the objective altitude, effectively widening the window the rocket needs to achieve.

The recovery analysis includes determining the velocities at which the two parachutes would be deployed, the impact velocity of the rocket as it lands on the surface, as well as the distribution of trajectories (as calculated by RockSim Pro). The approximated peak acceleration for the rocket is 158 ft./s². The drogue parachute deployment vertical velocity and altitude are 33 feet per second upward and 3100 feet respectively, neglecting the air brake effects. With the air



Figure 21: RockSim Pro Distribution of Uncertainty Trajectory Landing Sites

brake, the altitude and velocity would assuredly be lower so these numbers provide a conservative estimate. For the main parachute deployment the vertical velocity and altitude are 64 feet per second downward 790 feet respectively. This deployment altitude along with the 8-foot diameter parachute will decrease the rocket apogee safely to approximately 20 feet per second before ground impact.

The lattermost parameter in the recovery analysis is determining days before a test launch, the team looks at the launch conditions of the launch area as predicted by the National Weather Service. This includes everything from temperature and humidity, to wind magnitude and direction. Using these conditions in RockSim Pro, an uncertainty simulation can be used to generate potential landing sites of the rocket. This analysis has already been performed for the test launch on April 12th and a similar simulation will be carried out for the competition launch

on April 26th. The importance of this is to determine a probability field of where and if environmental issues come into affect such as the rocket landing near power lines. If these situations do occur in the data field, a single data point can be isolated and looked at for the characteristics that produced the abnormal result and, if possible, take action to mitigate said characteristics.

CONCLUSION

CySLI's current payload and rocket design will meet the competition directive calling for several measurement systems on a rocket flight to a required apogee. The Raspberry Pi computer will be utilized in the control of a variable-drag air brake system in order to achieve the 3000-foot target altitude. The air brake system, modeled in CFD, allowed for a more accurate solution to the rocket trajectory after motor burnout. Furthermore, multiple rocket simulation programs were used to approximate and validate the critical parameters in the launch vehicle performance. Conclusively, the thorough technical analysis performed by the team and the precautions taken in rocket construction will result in a safe and successful launch.

REFERENCES

- [1] Adafruit. *Adafruit Ultimate GPS Breakout - 66 Channel w/10 Hz Updates*. n.d. Image. 11 April 2014. <<http://www.adafruit.com/products>>.
- [2] Culp, Randy. *Rocket Equations*. 25 February 2007. Document. 9 April 2014. <http://my.execpc.com/~culp/rockets/rckt_eqn.html>.
- [3] Hexpert Systems. *ZLog-7*. n.d. Image. 11 April 2014. <<http://www.hexpertsystems.com/zlog/Z7/>>.
- [4] HobbyTronics. *MinIMU-9 V2 Gyro, Accelerometer, and Compass (L3GD20 and LSM303DLHC)*. n.d. Image. 11 April 2014. <<http://www.hobbytronics.co.uk/minimu-9>>.
- [5] Murray, Matthew. *PC Mag*. 13 July 2012. Image. 11 April 2014. <<http://www.pc当地.com/article2/0,2817,2407058,00.asp>>.

BUDGET

Capital Items	Cost / Item	Quantity	Total
PAYOUTLOAD EXPENSES -----			\$220.00--
RC Transmitter/Receiver	\$30.00	1	\$30.00
High-torque Servo			\$36.00
12V Battery Pack	\$22.25	1	\$22.25
AA Batteries			\$14.00
GPS Receiver	\$39.95	1	\$39.95
Raspberry Pi			\$39.95
Servo Control Board	\$14.95	1	\$14.95
Cobbler / Cable			\$7.95
Breadboard	\$5.00	1	\$5.00
USB to TLL Cable			\$9.95
ROCKET EXPENSES -----			\$1477.55--
Body Tubes (6 in.)	\$99.00	2	\$198.00
Nosecone			\$95.00
Payload Section	\$82.49	1	\$82.49
Raven Featherweight Altimeter			\$155.00
Motor Reload Kit (K400)	\$239.54	2	\$479.08
9V Battery			\$2.78
Drogue Parachute (34 in.)	\$25.15	1	\$25.15
Main Parachute (96 in.)			\$157.45
Kevlar Shock Cord (per yard)	\$4.13	20	\$82.60
3D Plastic Printing			\$200.00
TRAVEL EXPENSES -----			\$1070.20--
Mileage (1 vehicle x 15 passenger van x 490 mi round trip x \$0.58 /mi.)	\$284.20	1	\$284.20
Trailer (\$22/day x 3 days)			\$66.00
Hotel (4 rooms x 2 nights)	\$180.00	4	\$720.00
CAPITAL TOTAL			\$2767.75